ANL/CEN/FE-79-4

ANL/CEN/FE-79-4

LABORATORY SUPPORT FOR IN SITU GASIFICATION--REACTION KINETICS

Annual Report
October 1977—September 1978

by

J. E. Young, S. H. Wong, J. E. Johnson,
N. Sikand, and A. A. Jonke

ARGONNE NATIONAL LABORATORY, ARGONNE, ILLINOIS

Prepared for the U. S. DEPARTMENT OF ENERGY
under Contract W-31-109-Eng-38

DISCLAIMER

Printed in the United States of America
Available from
National Technical Information Service
U. S. Department of Commerce
5285 Port Royal Road
Springfield, VA 22161

NTIS price codes
Printed copy: A03
Microfiche copy: A01

Distribution Category:
Coal Conversion and Utilization—
Coal Gasification (UC-90c)

ANL/CEN/FE-79-4

ARGONNE NATIONAL LABORATORY
9700 South Cass Avenue
Argonne, Illinois 60439

LABORATORY SUPPORT FOR *IN SITU* GASIFICATION--REACTION KINETICS

Annual Report
October 1977—September 1978

by

J. E. Young, S. H. Wong, J. E. Johnson,
N. Sikand, and A. A. Jonke

Chemical Engineering Division

February 1980

Previous annual reports in this series

ANL-76-131	October 1975—September 1976
ANL/CEN/FE-79-1	October 1976—September 1977

THIS PAGE

WAS INTENTIONALLY

LEFT BLANK

TABLE OF CONTENTS

LIST OF FIGURES

LIST OF TABLES

LABORATORY SUPPORT FOR *IN SITU* GASIFICATION--REACTION KINETICS

October 1977—September 1978

by

J. E. Young, S. H. Wong, J. E. Johnson,
N. Sikand, and A. A. Jonke

ABSTRACT

This work is directed toward support studies for the national program for the development and demonstration of *in situ* coal gasification processes. The objective of this work is to determine the reaction-controlling variables and reaction kinetics for the gasification of chars obtained by pyrolyzing coal in simulated underground gasification conditions. The reactions being studied and to be studied include steam-char, CO_2-char, H_2-char, the water-gas shift reaction, and the methanation reaction.

In this report are presented data regarding the kinetics of the reaction of steam with chars prepared from Pittsburgh seam high-volatile bituminous coal. In addition, a reaction model is described correlating the steam-char reaction rates measured earlier for Hanna subbituminous coal with operating conditions including temperature, partial pressures of steam and hydrogen, and extent of carbon gasification. Partial results are presented and discussed for an investigation of structural parameters of Hanna char as a function of pyrolysis conditions and extent of carbon gasified.

SUMMARY

This work has the objectives of providing engineering data for process control and resource evaluation for underground coal gasification. Kinetic data for gasification of chars under simulated *in situ* processing conditions are provided. The coal samples studied are representative of coals at sites where field tests either are currently being conducted or are under consideration. Chars for gasification are prepared by pyrolyzing the coal under conditions characteristic of the *in situ* gasification process.

The reaction of steam with chars prepared from Pittsburgh seam high-volatile bituminous coal was determined for the temperature range, 700 to 850°C, and partial pressures of steam of 70-500 kPa (0.7-5 atm). In order to counteract the coking properties of this coal during pyrolysis, the coal was crushed to 30 mesh and diluted with three times its volume of 30 mesh α-alumina before being placed in the reactor. The reaction of steam with Pittsburgh char at lower temperatures (∿700°C) is approximately one order of magnitude slower than had been determined earlier for chars from Hanna subbituminous coal, and at higher temperature (∿850°C), Pittsburgh char is about one-third as reactive as Hanna char. Extensive micropore diffusion

limitations are observed with the diluted Pittsburgh char. At low temperatures (~700°C), this effect has about the same magnitude as the western subbituminous coals, as evidenced by the similarity of the apparent activation energies; E_a at 700°C, -44.9 kcal/mol for the Pittsburgh char and -43.5 kcal/mol for the Wyodak char. At high temperatures (~850°C), the apparent activation energy for the Pittsburgh char is -18.0 kcal/mol. This indicates that the steam-carbon reaction is very severely diffusion-limited--much more than was observed for either the Hanna char or the Wyodak char. The reaction of steam with the Pittsburgh char is very close to first order in steam for the range of steam partial pressures investigated.

A rate expression has been derived in which experimentally determined rates of reaction of steam with Hanna char have been correlated with the operating variables in the ranges of interest for *in situ* gasification. This expression has the form

$$r_c = \frac{kX_c^{0.59}P_{H_2O}^{0.56}}{1 + KP_{H_2}^2}$$

where

r_c = rate of gasification of the ash-free carbon, h^{-1}

X_c = fraction of ash-free carbon gasified

k = reaction rate constant = $2.04 \times 10^4 \exp(-25940/RT)$, $kPa^{-0.56}\ h^{-1}$

P_{H_2O} = partial pressure of steam, kPa

K = adsorption rate constant = $8.87 \times 10^{-13} \exp(38350/RT)$, kPa^{-2}

P_{H_2} = partial pressure of hydrogen, kPa

This expression fits the experimental data with a maximum deviation of approximately 30%. The greatest errors occur at high temperatures.

Earlier studies with western subbituminous coals indicated that reaction rate is strongly dependent on the amount of carbon removed from the char. An investigation has been initiated to determine the pore structure and surface area of chars as a function of carbon removal. At 750°C, removal of 65% of the carbon from Hanna char has been found to increase its surface area sixfold. Simultaneously, the volume of pores having diameters greater than 60 Å increases approximately fourfold and the reaction rate increases approximately threefold. This work is not yet complete, but it is planned to use this information in obtaining an improved correlation of reaction rate with extent of carbon gasification.

I. INTRODUCTION

Current and predicted shortages of gaseous fuels in this nation have led to increased effort to develop processes for the underground conversion of coal to cleaner fuels, either for combustion or for use as petrochemical feedstocks. The concept of *in situ* coal gasification has been investigated intermittently in the U.S.A. and European countries since the early part of this century. Extensive testing of the concept has been carried out in the U.S.S.R. However, underground gasification development has been interrupted in the past either by war or by alleviation of the need of such technology due to the discovery of extensive natural gas reserves, as in the case of the Soviet Union. The increased interest in underground gasification in this country can be attributed to rapidly declining reserves of inexpensive natural gas and the search for alternative sources of gaseous fuels for industries which cannot be converted economically from gaseous to solid fuel feeds.

During gasification of coal underground, three distinct reaction zones can be identified. In the first zone, there is drying and pyrolysis (devolatilization) of the coal. Following the pyrolysis zone is the reduction zone where a significant portion of the char produced in the devolatilization zone is gasified. Major reactions here are the reactions of char with steam and carbon dioxide. Carbon dioxide is produced in the third zone by combustion of the remaining char in air or oxygen injected into the coal seam. The heat for the process is generated in the combustion zone and is carried into other zones by the flow of the hot gaseous products of combustion through pores and fissures generated in the coal during pyrolysis.

The characteristics of various reactions in *in situ* gasification processes are very important. An understanding of them is especially important if *in situ* gasification is to be employed to produce a variety of products and if a variety of coal sources is to be used. Petrochemical feedstocks, combined cycle power generation, and pipeline gas production will require gases of different compositions, and each application could make good use of products of *in situ* gasification.

In addition to studies relating reaction behavior to subsequent product gas compositions, global mathematical models must be developed to permit (1) calculation of the efficiencies of the process, (2) prediction of the rates of movement of the various reaction zones during *in situ* gasification, (3) specification of optimum process configurations and parameters, and (4) prediction of the effects of processing upsets (*e.g.*, massive subsidence into the reaction zone). For a model to be useful, it should be capable of describing the time and spatial dependence of the gasification processes as they occur underground. Furthermore, effective mathematical models can be used to determine how variables such as air injection rate, water infusion, and steam partial pressure can be adjusted to tailor the product to the needs of the consumer. Not all of those capabilities have yet been included in current models for *in situ* gasification, but refinements will be made to permit the global models to be used to meet these as well as other goals.

All of the global mathematical models are currently limited in utility because there is a lack of kinetic data for the primary reactions involving coals of interest for *in situ* gasification. The reaction of carbon with

oxygen is very rapid, and differences in the physical and chemical nature of the chars and coals have minor effects on the rates of this reaction. However, chars obtained from different coals and at different pyrolysis conditions by *in situ* pyrolysis with steam, carbon dioxide, or hydrogen vary in reactivity. Little information on these reactions is available in the literature for chars prepared (1) from coals important in underground gasification and (2) under conditions similar to those encountered underground.

The purpose of our work at ANL is to obtain kinetic information that is directly applicable to mathematical models for *in situ* gasification. These studies will allow the important processing variables in underground gasification to be identified. The coals being utilized are similar to those used in current field tests or proposed for use in commercial underground gasification. The processing conditions surveyed include those expected to be encountered in *in situ* gasification.

The kinetics of the reaction of oxygen with carbon is not included in our work. As stated above, this reaction is rapid, and the results obtained in the mathematical models are quite insensitive to errors in the rate constants for this reaction. The reactions being studied in this program include:

$$H_2O + C \rightleftarrows H_2 + CO$$

$$CO_2 + C \rightleftarrows 2CO$$

$$2H_2 + C \rightleftarrows CH_4$$

$$H_2O + CO \rightleftarrows H_2 + CO_2$$

$$3H_2 + CO \rightleftarrows CH_4 + H_2O$$

Only the first three of the above reactions contribute directly to conversion of char to gaseous products. The final two reactions affect the composition of the product gases and are of considerable economic importance in relation to tailoring the product gas to the needs of various industries which would make use of the end products of *in situ* gasification.

Variables being investigated in this study include total pressure, reaction temperature, coal devolatilization conditions, and partial pressure of steam. Kinetic data to be obtained include rate constants, reaction orders with respect to each of the reactants, and apparent activation energies. These parameters are being determined for bituminous coal from the Pittsburgh seam and have been determined for subbituminous coals from Wyodak and Hanna seams of Wyoming.

In this annual report, kinetic data for the reaction of steam with chars prepared from Pittsburgh seam high-volatile bituminous coal are presented. Also discussed is a reaction model currently proposed for correlation of data obtained using Hanna subbituminous coals. The reaction rate data have been reported in earlier reports of this series. Also included are the results of a study with Hanna char relating the pore structure and surface area of this char to extent of gasification.

II. EXPERIMENTAL

The kinetics studies are carried out in a packed bed differential reactor in which steam, carbon dioxide, and/or other reactants are blended with nitrogen to obtain the desired total pressure and partial pressures of reactants. The experimental apparatus and general operating procedures have been described in detail.[1]

Pyrolysis of the char is carried out just before gasification in the gasification reactor under conditions of pressure, heating rate, and sweeping gas composition similar to those encountered in underground gasification. Because of its coking properties, the Pittsburgh seam coal is diluted with three parts by volume of α-alumina as is discussed below.

The Pittsburgh coal is crushed to -25 +35 mesh and is mixed with the 30-mesh alumina before placement in the reactor. This procedure differs from that used in the earlier studies with Western subbituminous coals, in which the coal was crushed to -4 +12 mesh and placed directly in the reactor without dilution. Pyrolysis conditions used here were similar to those used for the subbituminous coals: 3°C/min heating rate up to the reaction temperature, a total system pressure of approximately 800 kPa (100 psig), and a sweeping gas consisting of 20% hydrogen in nitrogen flowing at a rate of 1.0-1.5 L/min STP.

III. RESULTS AND DISCUSSION

A. Steam-Char Reaction Kinetics--Pittsburgh Seam Coal

If a coking coal such as Pittsburgh coal is pyrolyzed in our reactor system without inert diluent, interparticle contact during pyrolysis results in fusion of the coal into a solid mass and accessibility of steam to the char is severely limited. At approximately 400°C, the coal becomes very plastic and begins to fuse. In our reactor, this results in an increase of pressure drop across the coal bed. By the time the reactor has heated to 525°C, gas flow through the bed has decreased to <10% of the orginial value, with occasional complete blockage of gas flow. At about 550°C pyrolysis of the liquid phase proceeded to the extent that the fused mass began to shrink away from the walls of the reactor tube, permitting unrestricted gas flow around the perimeter of the single lump of coke. This shrinkage continued throughout pyrolysis until the final temperature for reaction was reached.

Because of this shrinkage channeling of the reactant steam around the coke was extensive with very little of the steam passing through the mass. In effect, reaction is primarily limited to the outer surface of a large single particle of coke; hence, the apparent reaction rate is considerably less than that expected for very small char particles. The purpose of the α-alumina is to prevent interparticle contact during the pyrolysis phase of the experiment and thus prevent formation of a single mass of coke. Adding the inert diluent probably gives a better approximation of the intrinsic kinetics for the Pittsburgh char, for which the only diffusion limitations to reaction would be internal and would depend on the particles' actual pore size distribution. Since isolation of coal particles would not be encountered in actual underground conversion of a coal having a high swelling index, the mass transport limitations occurring underground due to swelling of the coal would have to be characterized and be included in the global mathematical model to predict the appropriate profile of partial pressures of steam and reaction products. This predicted profile of reaction conditions could then be combined with the intrinsic kinetic data to form a physically realistic reaction model for simulation.

In Figs. 1-4 are plots of the rates of reaction of steam with diluted char prepared from Pittsburgh bituminous coal in the temperature range of 700-850°C and with a partial pressure of steam of approximately 230 kPa (2.3 atm). At 700°C (Fig. 1), only a very small fraction of the char reacts with the steam and by the time 20% of the carbon has been gasified, the reaction rate has decreased to an insignificant value. A similar phenomenon had been observed in the case of both Wyodak and Hanna Western subbituminous coals at low reaction temperatures.[2] With these lower rank coals, approximately 5% of the char exhibited a relatively high reactivity at 600°C, while the remaining char exhibited a reduced, but measurable rate.

The reaction rate of Pittsburgh char with steam at 600°C was too low to permit accurate determination. Consequently, the lowest temperature for our data analysis is 700°C. It should be noted that even at 700°C (Fig. 1), the residual char after 20% gasification was so unreactive that the reaction rate could not be measured.

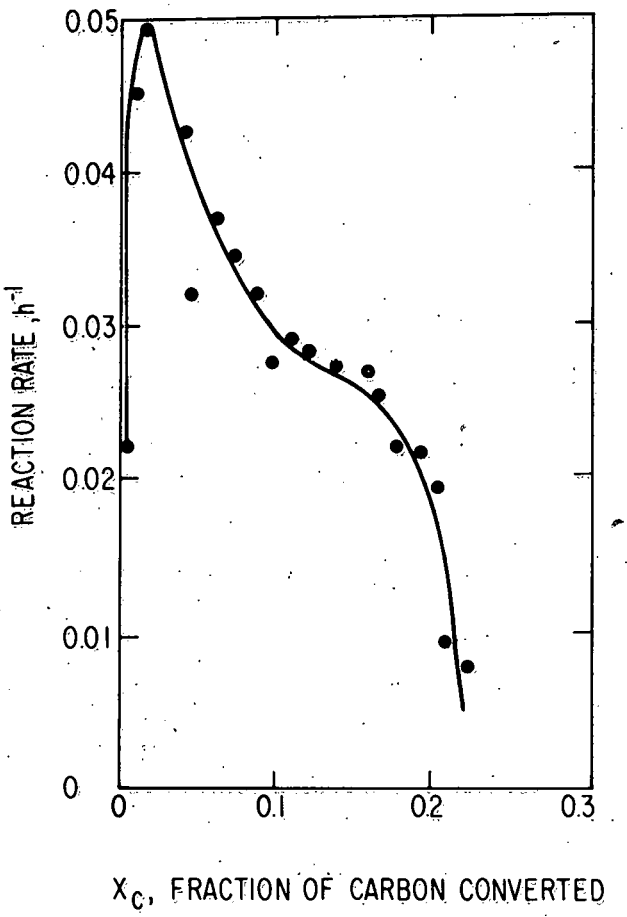

Fig. 1. Reaction Rate with Steam *vs.* Percent Carbon Conversion for Diluted Pittsburgh Seam Char. 700°C, 230 kPa (2.3 atm), Steam.

At 750°C (Fig. 2), the reaction rate *vs.* carbon conversion plot is completely different from the Fig. 1 plot. There is no high initial reactivity, as had been observed at 700°C (Fig. 1). In addition, slow-opening of the pore structure of the char that had been observed for the Western chars[2] did not occur with the Pittsburgh char. By the time 15% of the carbon had been gasified, the reaction rate reached a maximum; next, there was a very slow decrease in reaction rate until seventy percent was gasified; then the rate decreased rapidly. At higher temperatures (Figs. 3 and 4), the reaction rate reached a maximum at about 20% carbon conversion and remained relatively constant (within a ±30% band) until nearly all of the carbon was consumed.

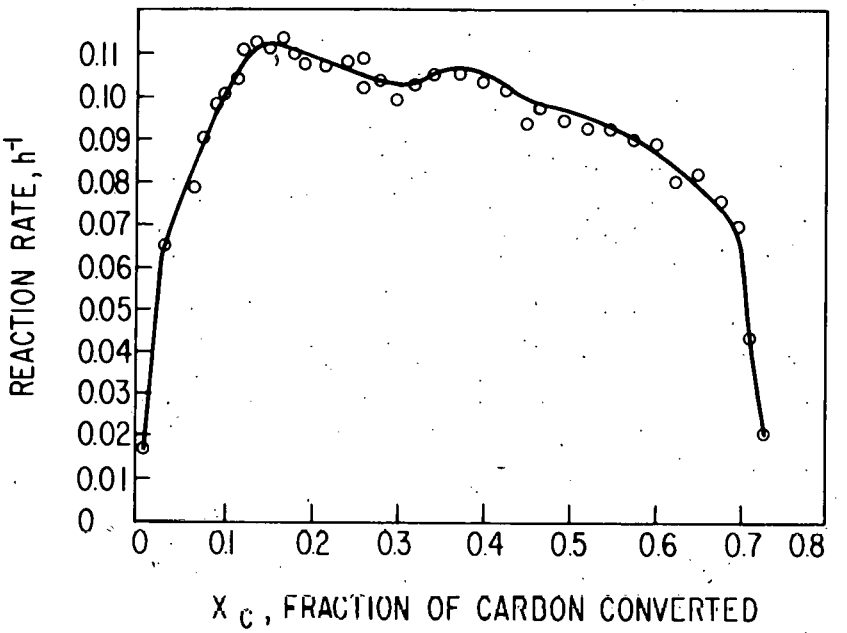

Fig. 2. Reaction Rate with Steam *vs.* Percent Carbon Conversion for Diluted Pittsburgh Seam Char. 750°C, 240 kPa (2.4 atm), Steam.

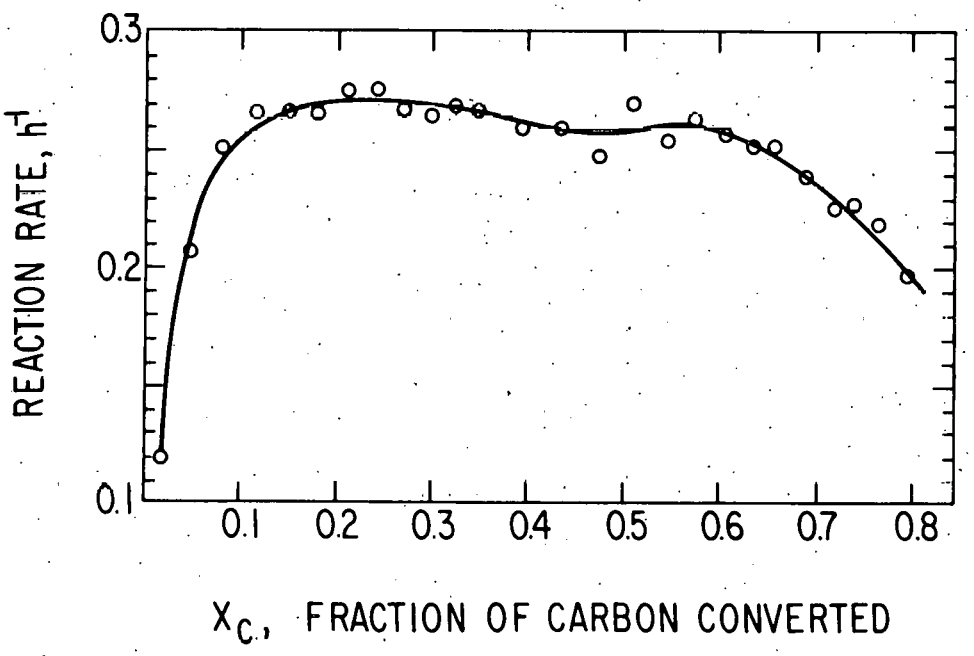

Fig. 3. Reaction Rate with Steam *vs.* Percent Carbon Conversion for Diluted Pittsburgh Seam Char. 800°C, 230 kPa (2.3 atm), Steam.

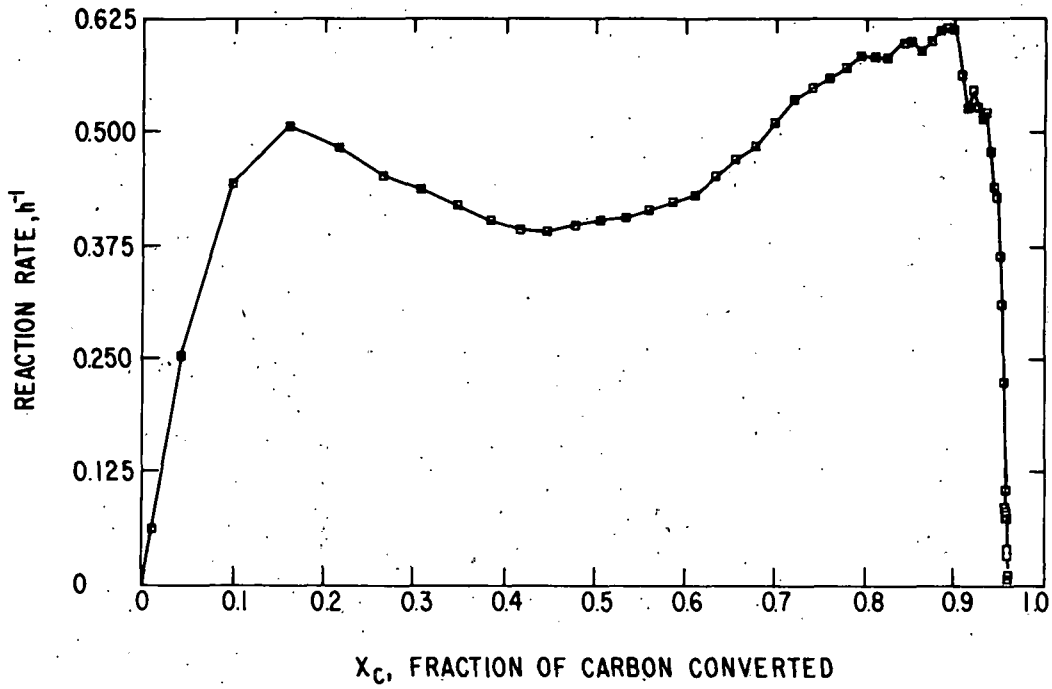

Fig. 4. Reaction Rate with Steam *vs.* Percent Carbon Conversion for Diluted Pittsburgh Seam Char. 850°C, 230 kPa (2.3 atm), Steam.

The temperature dependence of the reaction rate for steam with the Pittsburgh seam char is shown in Fig. 5. The solid curve corresponds to the data obtained for coal diluted with alumina. For each temperature, the rates at 10, 20, 30, and 50% carbon conversion are plotted. The slope of the Arrhenius curve for this char does not show the dependence upon extent of carbon conversion which was observed earlier with the Western coals.[2] This is consistent with the different shapes of the reaction rate *vs.* carbon conversion curves (Figs. 1-4) discussed above.

Extensive limitations to the steam-carbon reaction caused by slow micropore diffusion are observed with the diluted Pittsburgh char. At low temperatures, this effect is quite small, the apparent activation energy (E_a) being -44.9 kcal/mol at 700°C. This value closely approximates the value obtained for the Wyodak subbituminous coal (E_a = -43.5 kcal/mol).[2]

At high temperatures (~850°C), the apparent activation energy for the diluted Pittsburgh char is -18.0 kcal/mol, indicating that the steam/carbon reaction is severely diffusion-limited--much more than was observed for either the Hanna char or the Wyodak char. Apparently, the micropore structure of the Pittsburgh bituminous char does not open up as readily as that of the Western subbituminous chars.

In summary, the reaction of steam with the Pittsburgh char at lower temperatures is approximately one order of magnitude slower than for the Hanna char; at higher temperatures, the Pittsburgh char is about one-third

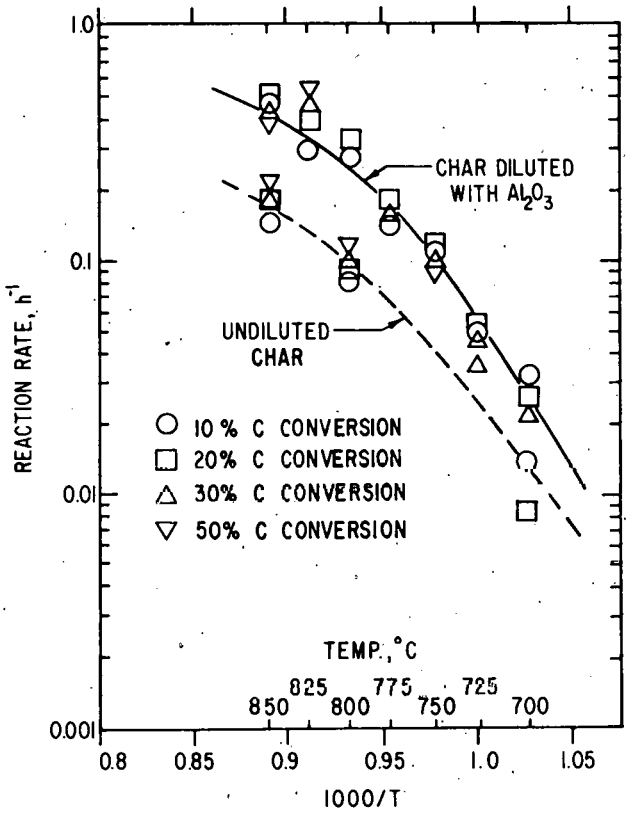

Fig. 5. Temperature Dependence of Steam-Char Reaction Rate with Pittsburgh Seam Char and 230 kPa Steam.

as reactive with steam. The reason for this difference is most probably significant differences in the physical structures of the two ranks of coal.

In order to investigate the effects of the alumina dilution upon our data, a short series of runs was made without alumina. Pittsburgh coal crushed to -25 +35 mesh was placed in the reactor and pyrolyzed under our standard conditions, permitting a single lump of coke to form in the reactor; there was a high degree of channeling of steam during gasification. The apparent reaction rates for the undiluted coke were determined at 850, 800, and 700°C and are shown in Fig. 5. With this experimental procedure, the reaction rate was approximately one-third that observed with the diluted char. In addition, the temperature dependence was somewhat less than that for the diluted char. The data also indicated a dependence of E_a upon the extent of carbon conversion, similar to that observed for the Western subbituminous coals, although insufficient data were obtained to make a definite conclusion.

The reactor configuration used in this study of undiluted char is most likely a rather poor simulation of actual processing conditions for *in situ* gasification. Nevertheless, measurements from this experimental series should provide an estimate of the extent to which reaction rate is limited by bulk mass transfer diffusion in a coking coal.

Figure 6 shows the dependence of the rate of reaction on the partial pressure of steam. This experimental series was carried out with the steam pressure ranging from 86 to 470 kPa (0.86 to 4.6 atm). The $\log_{10}$ of the reaction rate is plotted as a function of the $\log_{10}$ of the steam partial pressure for 10 and 50% carbon conversion. A slope of this logarithmic plot would yield the reaction order with respect to steam.

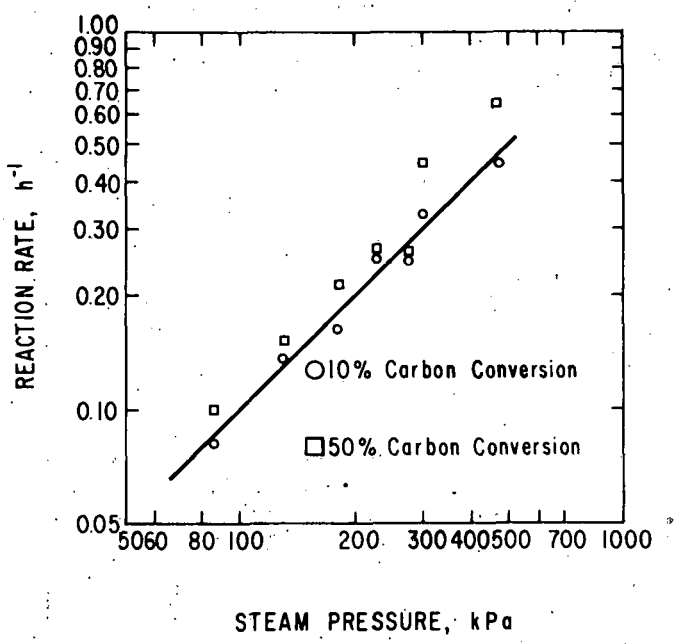

Fig. 6. Dependence of Reaction Rate on Partial Pressure of Steam. Pittsburgh Seam Char. 800°C. The solid line corresponds to first order dependence.

For the range of steam partial pressures studied, reaction with steam is approximately first order for the Pittsburgh seam coal (line in Fig. 6). This contrasts with a reaction order of 0.85 measured for the Wyodak coal and 0.56 measured for the Hanna coal in the same range of steam partial pressures. The reaction order decreased to nearly zero at high steam partial pressures in the case of the Wyodak coal, and there are indications that the same trend would exist with the Pittsburgh seam coal.

The range of partial pressures of steam studied for the three coals above is in approximately the range expected for actual underground gasification. If necessary, extrapolation of these data to lower partial pressures of steam would be permitted because the reaction order appears to be quite similar in all three cases. Extrapolation to higher partial pressures, however, would be very inadvisable because the reaction order might decrease at these higher pressures. For the relatively shallow, low-pressure field

operations currently under way and envisioned in the near future, it is highly unlikely that the partial pressure of steam would increase above 3 atm, except possibly in very localized areas of rapid water intrusion. On the average, across the entire reaction front, the partial pressure of steam would probably be 1 atm or less.

Figure 7 shows the inhibitive effect of hydrogen on the steam-char reaction at 800°C for Pittsburgh char. The reaction rate was measured at 30% carbon conversion with a partial pressure of steam of 2.35 to 2.50 atm. Data for the Hanna coal char at the same operating conditions are also presented to allow comparison.

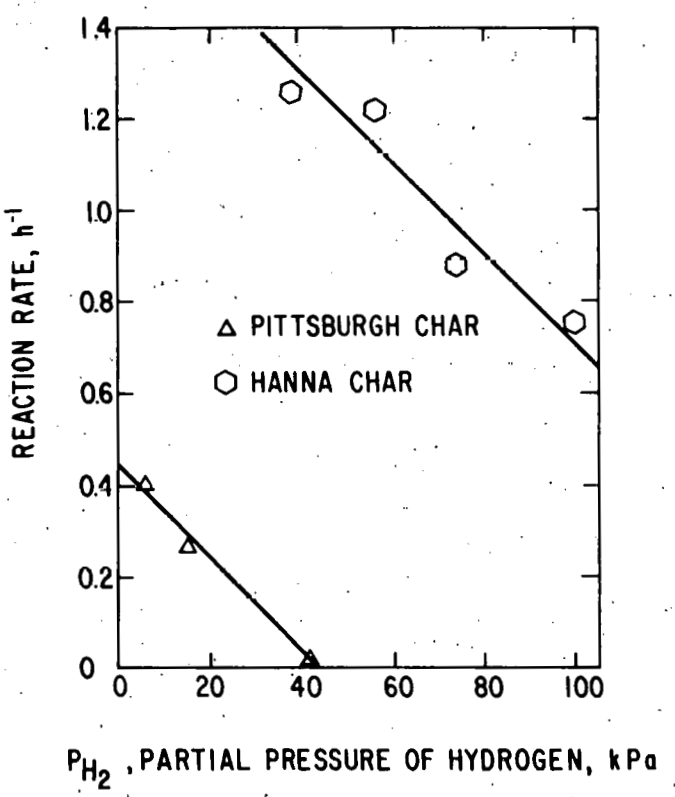

Fig. 7. Hydrogen Inhibition of the Steam-Char Reaction. 800°C, 30% Carbon Conversion, 235-250 kPa Steam.

Additional data regarding inhibition by hydrogen of the reaction of steam with Pittsburgh char must be obtained. The reaction rates and concentrations of product gases are so low that it was necessary to upgrade the gas analytical system in our experimental reactor for accurate measurement. This has now been completed, and these data will be obtained soon.

B. Modeling of the Steam-Char Reaction for Hanna Coal

When steam reacts with char, it is generally accepted that the primary reaction is:

$$C + H_2O \rightleftharpoons CO + H_2 \quad (1)$$

Any carbon dioxide produced in the system is attributed to the water-gas shift reaction:

$$CO + H_2O \rightleftharpoons CO_2 + H_2 \quad (2)$$

This CO_2 may subsequently react with the char to form carbon monoxide as follows:

$$C + CO_2 \rightleftharpoons 2CO \quad (3)$$

Methane is also produced in small but measurable quantities. The main reactions for its formation are believed to be

$$C + 2H_2 \rightleftharpoons CH_4 \quad (4)$$

$$CO + 3H_2 \rightleftharpoons CH_4 + H_2O \quad (5)$$

However, the above two reactions generally occur so slowly that they do not make a significant contribution to overall gasification rate.

Of the above-mentioned five reactions, only reactions 2 and 5 do not contribute to the direct conversion of char to gaseous products. Dependent upon the nature of impurities present in the ash components of the raw coal, Eq. 2 can rapidly approach equilibrium, as was found in earlier work at ANL and elsewhere.[3,4] It should be noted that reactions 2 and 5 affect the product composition, but do not contribute to the overall carbon conversion rate.

Although many studies have been made of the carbon-steam reactions,[5,6] difficulties generally arise from the fact that one must deal with a reaction network consisting of at least five simultaneous reactions (1-5). Furthermore, the nature and chemical composition of the raw coal and char[7] contribute added complications to the kinetic studies of these reactions. The latter variables undoubtedly play a significant role when a wide variety of coals are studied but are generally ignored in this analysis--since coal samples collected in this investigation are limited to a given seam and the chars prepared for each gasification run are treated similarly to minimize variations. A possible exception to this assumption of uniform character is demonstrated in our recent surface area and pore size measurement studies. This physical variation of char structure during gasification and its possible implication to the overall reaction rate are discussed in a later section of this report.

In our earlier attempts[8] to correlate the kinetic data for Western subbituminous coal, it was found that neither a simple power function nor a first order Langmuir-Hinshelwood kinetic model provided results that account satisfactorily for the severe hydrogen-inhibition effect in the

char-steam reaction. Consequently, a substantial effort was expended this year on the construction of a gasification rate model that could adequately describe the kinetic behavior for the Hanna char.

Table 1 shows the six models that were tested for their fit with our kinetic data for Hanna. These models assumed that the reaction rate is n-order dependent with respect to the partial pressure of steam, P_{H_2O}, and is a function of the partial pressure of product hydrogen, P_{H_2}. For Hanna coal, n equals 0.56.

Table 1. Models Tested for Correlation with Experimental Results

Model	Rate Expression[a]		Model	Rate Expression[a]	
I	$r_c = \frac{k_I P_{H_2O}^n}{1 + K_I P_{H_2}}$	(6)	II	$r_c = \frac{k_{II} P_{H_2O}^n P_{H_2}}{1 + K_{II} P_{H_2}}$	(7)
III	$r_c = \frac{k_{III} P_{H_2O}^n}{1 + K_{III} P_{H_2}^2}$	(8)	IV	$r_c = \frac{k_{IV} P_{H_2O}^n P_{H_2}}{1 + K_{IV} P_{H_2}^2}$	(9)
V	$r_c = \frac{k_V P_{H_2O}^n}{(1 + K_V P_{H_2})^2}$	(10)	VI	$r_c = \frac{k_{VI} P_{H_2O}^n P_{H_2}}{(1 + K_{VI} P_{H_2})^2}$	(11)

[a] Nomenclature

- r_c = rate of gasification of the ash-free carbon
- k_i = reaction rate constant for model i
- P_{H_2O} = partial pressure of steam, atm
- K_i = adsorption rate constant for model i
- P_{H_2} = partial pressure of hydrogen, atm

Measurements of the overall reaction rate were made for partial pressures of steam ranging from 107 to 270 kPa (1.07-2.7 atm) and temperatures between 650 and 800°C. The partial pressure of hydrogen, which varied in each set of our experiments (15-100 kPa, 0.15-1.0 atmosphere), was adjusted externally in each run by adding a measured quantity of hydrogen gas at the reactor inlet. The raw reaction rate data obtained in these experiments have been reported earlier.[2]

In our experiments, an excess of steam is generally used, with its consumption rate during gasification not exceeding 10% of its inlet concentration. In addition, the system is operated at sufficiently high gas velocities to minimize external mass transfer effects and at small enough particle sizes to reduce internal mass diffusion effects.

In a differential reactor, the partial pressures of any gases vary little along the reactor. Thus, one may assume that the product gas compositions at the system outlet also represent point conditions within the reactor.

Three criteria were used to identify those models that provide a reasonable correlation with all kinetic data generated for Hanna:

1. The value of the coefficient of correlation for each set of experimental runs at given T, P_{H_2O}, and range of P_{H_2}.

2. The signs of the rate constants (k_i and K_i). Any models yielding negative values for either k_i or K_i are not further analyzed since they could provide no physical insight to a plausible mechanism.

3. The Arrhenius plot correlated for the two rate constants of each model over the range of temperature between 650 and 800°C. Models showing large scattering in calculated values of the rate constants are excluded from further consideration.

To calculate the two rate constants for each of the six models in Table 1, their variables could be rearranged in such a manner that a linear plot between two parameters in the X- and Y-axes can be made. For example, in the model

$$r_c = \frac{k_{III}\, P^n_{H_2O}}{1 + K_{III}\, P^2_{H_2}} \tag{8}$$

the terms r_c, $P^n_{H_2O}$, and P_{H_2} can be rearranged to obtain

$$\frac{P^n_{H_2O}}{r_c} = \frac{1}{k_{III}} + \frac{K_{III}}{k_{III}} P^2_{H_2} \tag{12}$$

If the model is an adequate representation of the kinetic data, the plot of experimental data for $P^n_{H_2O}/r_c$ and $P^2_{H_2}$ should be linear. From this plot, k_{III} and K_{III} which appear in Eq. 12 could be calculated from the intercept and slope of the line.

Of the six models, none appears to fit data obtained in any given set of experiments. Table 2 shows calculated values of their coefficients of correlation. The reaction conditions analyzed were for T = 700°C, P_{H_2O} ∿250 kPa

Table 2. Calculated Coefficients of Correlation for the Six Models Listed in Table 1

	Model					
Run	I	II	III	IV	V	VI
84	0.6146	-0.5951	0.6201	0.8634	0.6306	0.8846
101	0.2694	-0.2586	0.2778	0.3431	0.2632	0.3274
102	0.5562	-0.5614	0.5834	0.6019	0.5843	0.6043
103	-0.0960	0.0931	-0.0970	-0.0322	-0.0448	0.0239
104	-0.0583	0.0404	-0.0670	0.1268	-0.0200	0.1833

(2.5 atm), and P_{H_2} between 17 and 71 kPa (0.17-0.71 atm). The negative sign appearing prior to some of the coefficients in Table 2 indicates negative values for either k_i or K_i. In this effort, the effect of the fraction of carbon conversion (X_c) was not included in the rate expressions. Correlation quickly broke down at low X_c values for the six models tested. Disagreement is most significant at the midrange of P_{H_2}.

To improve the correlation, the effects of an X_c term on the values of the two rate constants were investigated. The values of reaction rate and adsorption rate constants were evaluated at constant X_c values between 0.1 and 0.5 and at various temperatures (650-800°C). The reaction rate and adsorption rate constants were evaluated for constant values of X_c using the three criteria established for model discrimination, and only Model III, Eq. 7, appears to fit with our data satisfactorily. Figures 8 and 9 show results of our correlation, using Model III. The coefficient of correlation calculated for each set of these points generally exceeds 0.9.

Figure 10 shows the k_{III} and K_{III} values as a function of X_c. The value of k_{III} shows a strong dependence on carbon conversion for the temperatures investigated, while values for K_{III} are, in general, relatively insensitive to any changes in X_c values. There are now reasons to believe that a rise in k_{III} value (or char reactivity) such as is shown in Fig. 10 results from pore structure enlargement providing additional surface area for reaction. In the absence of a complete set of pore volume measurements and surface area data, we speculate that perhaps there is a direct correlation among surface area, reaction rate constant (k_{III}), carbon conversion (X_c), and/or pore diameter. With this in mind, we postulate that the k_{III} values calculated previously are really

$$k_{III} = k\ f\ (X_c,\ T,\ P_i,\ ....) \qquad (13)$$

where k is the Arrhenius function and f (X_c, T, P_i, ...) is a function relating changes in surface area during reaction with X_c, temperature, partial pressure of reactant and/or product gases, as well as other factors such as mineral content and coal rank. It should be noted that T and P_i in Eq. 13 reflect the effects of these variables on the physical structure during pyrolysis, rather than the chemical and temperature effects on the reaction rate.

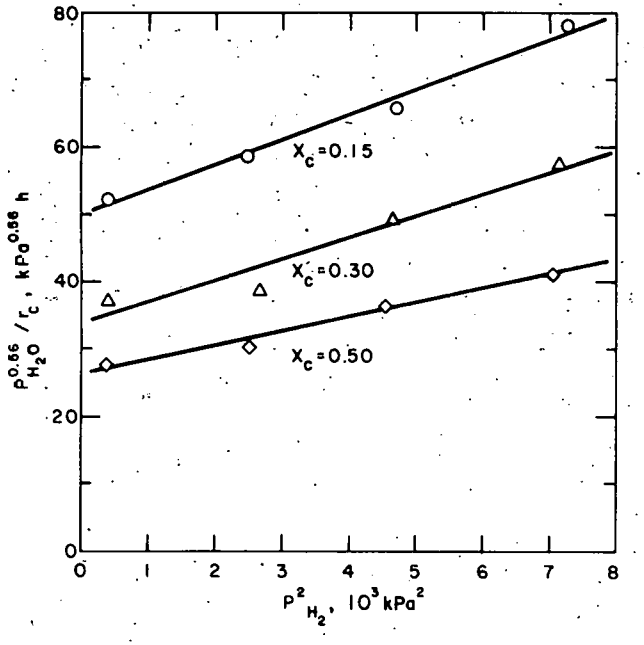

Fig. 8. Correlation of Experimental Results for Hanna No. 1 Char with Model III. T = 750°C, P_{H_2O} ≃ 2.5 atm, P_{H_2} = 0.20–0.85 atm.

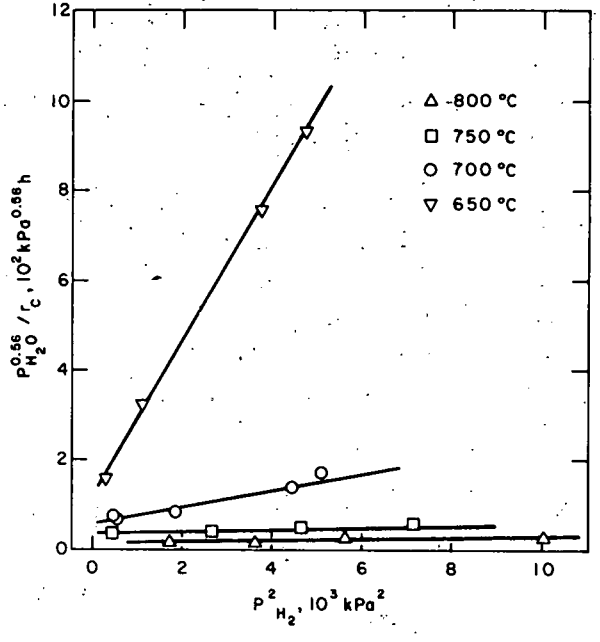

Fig. 9. Correlation of Hanna Char Experimental Data with Model III. P_{H_2O} ≃ 2.50 kPa, P_{H_2} = 15–100 kPa, X_c = 0.3.

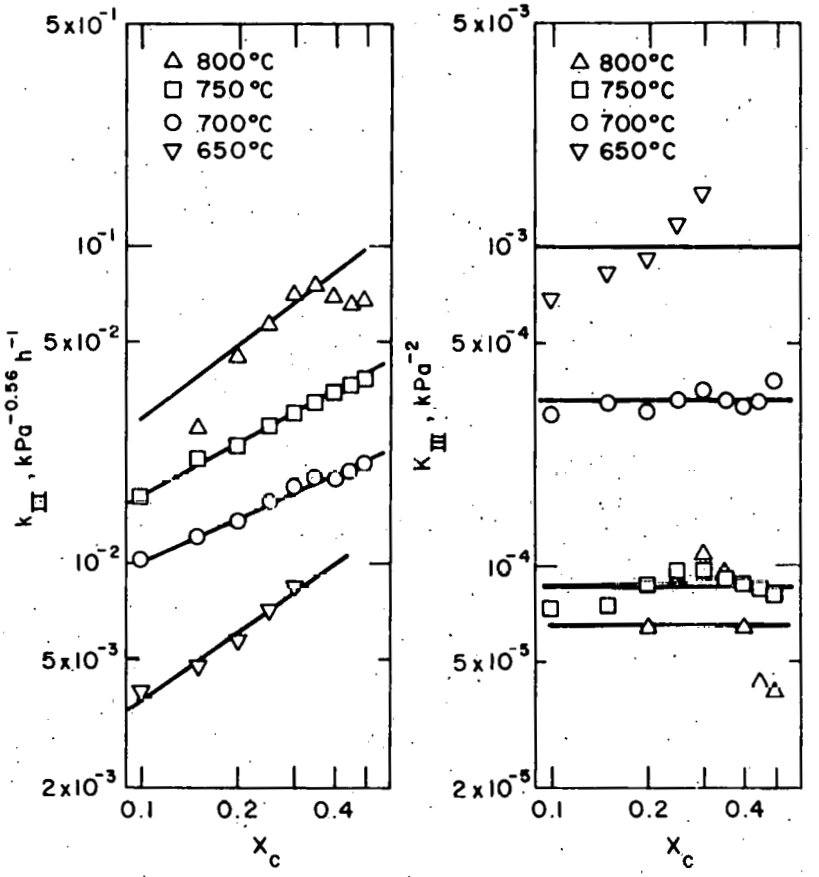

Fig. 10. Dependence of Rate Constants on X_c, Fraction of Carbon Converted. Hanna Char.

For simplicity in this analysis, it is assumed that

$$f(X_c m\ T,\ P_i, \ldots.) = X_c^m \tag{14}$$

Figure 10(a) also shows the results of our correlation using the above equation. Values of k_{III} and m were estimated from the slope and intercept of the line.

By assuming that both rate constants follow the Arrhenius relation, both the pre-exponential constants and the activation energies of k and K can be estimated. Figure 11 is an Arrhenius plot of the two rate constants *vs.* 1/T.

The model currently being considered has the form

$$r_c = \frac{k\ X_c^m\ P_{H_2O}^n}{1 + K\ P_{H_2}^2} \tag{15}$$

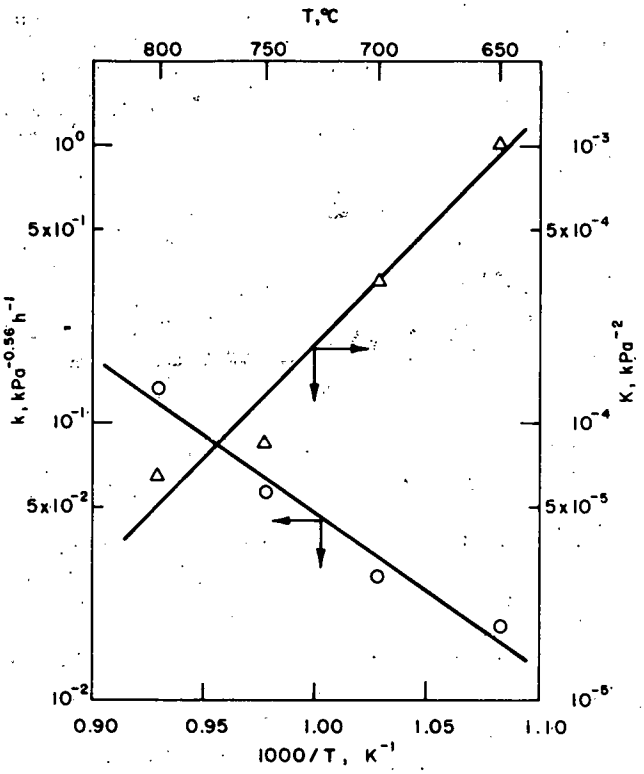

Fig. 11. Variation of Reaction Rate Constants with Temperature. Hanna Char.

where: $k = 2.04 \times 10^{4} \exp(-25940/RT)$, $kPa^{-0.56}\ h^{-1}$

$K = 8.87 \times 10^{-13} \exp(38350/RT)$, kPa^{2}

$m = 0.59$

$n = 0.56$

These values were obtained in linear fit with the kinetic data. The fits cover the range of 0.1-0.5 in X_c, 650-800°C in T, 15-100 kPa (0.15-1.0 atm) in P_{H_2}, and 250 kPa (2.5 atm) in P_{H_2O}.

Figures 12-15 show results of our comparison of the predictive capability of our model and a range of experimental points. Accuracy to within ±30% can generally be obtained. Deviations of the observed from the predicted reaction rates are most significant at the two extremes of the X_c range (Fig. 15) and are also very pronounced at the high reaction temperature (800°C, Figs. 12-14).

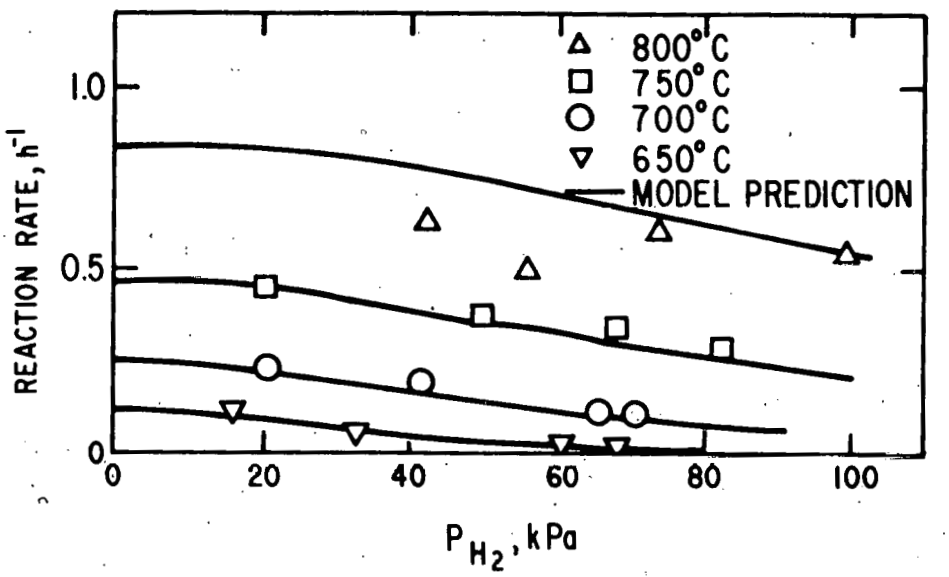

Fig. 12. Effect of Hydrogen Partial Pressure on Reaction Rate of Hanna Char at X_c = 0.15 and P_{H_2O} ≈ 250 kPa

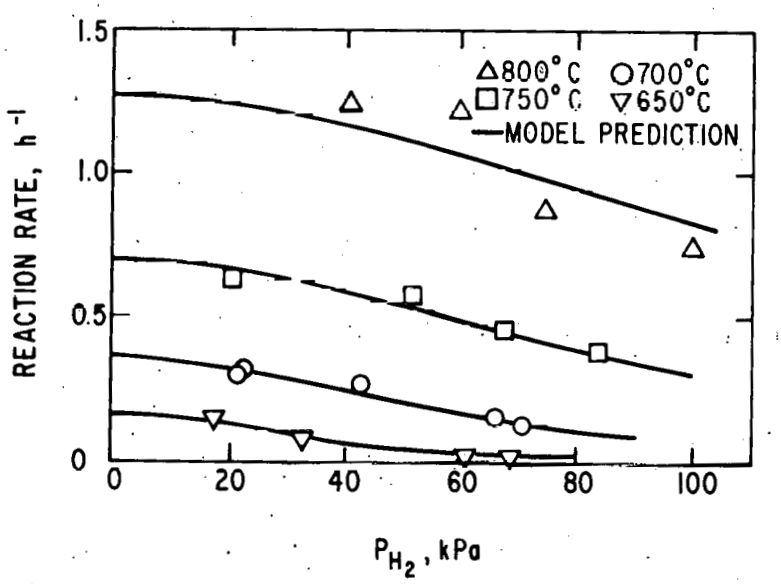

Fig. 13. Effect of Hydrogen Partial Pressure on Reaction Rate of Hanna Char at X_c = 0.3 and P_{H_2O} ≈ 250 kPa

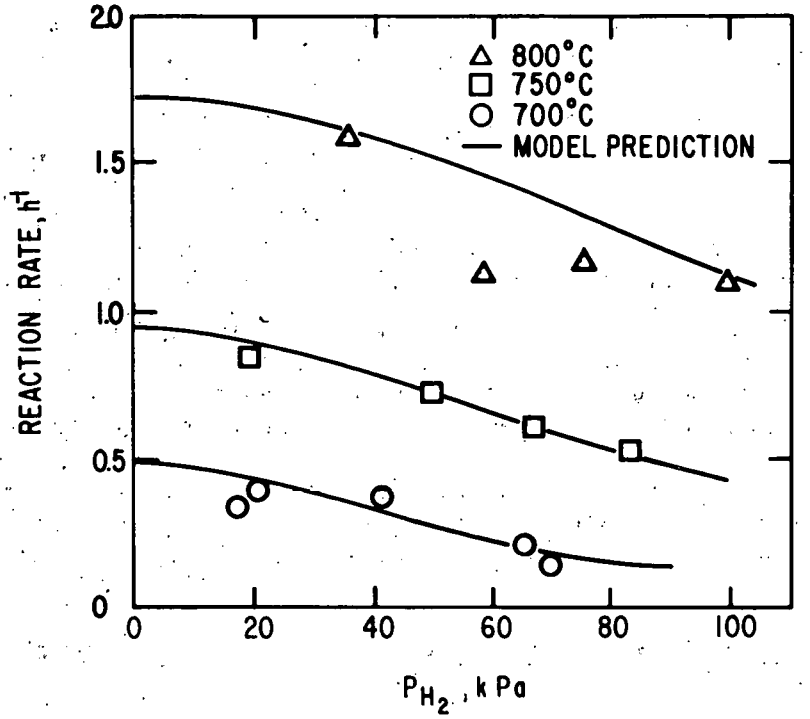

Fig. 14. Effect of Hydrogen Partial Pressure on Reaction Rate of Hanna Char at X_c = 0.5 and $P_{H_2O} \simeq$ 250 kPa

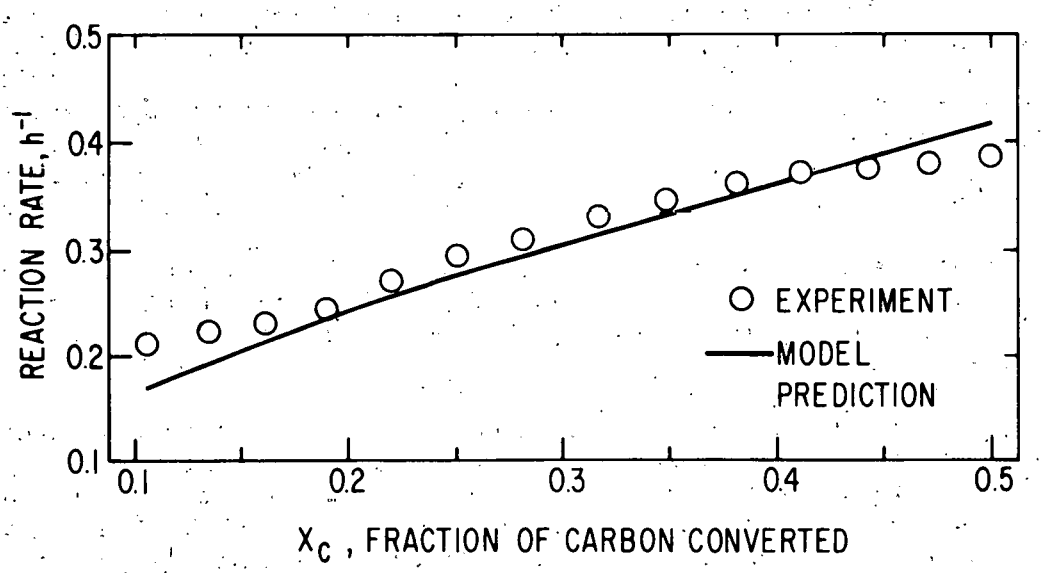

Fig. 15. Comparison of Observed and Predicted Carbon Conversion Rates for Hanna No. 1 Char. T = 700°C, P_{H_2O} = 250 kPa, P_{H_2} = 20-22 kPa, Run No. 104

Perhaps the most puzzling set of data is seen in Fig. 14 for T = 700°C. A closer look at reaction rates at this range of pressures may reveal another curve shape in which a maximum in r_c occurs at an intermediate value of P_{H_2}. The fact that Eq. 14 has improved the correlation of our data does not entirely eliminate this possibility. Work is currently under way to determine whether a maximum reaction rate does occur in the range of P_{H_2} between 0.2 and 0.4 atm.

The form of our presently proposed model is not the same as those proposed by any previous investigators. The second order dependence in P_{H_2} (in contrast to a first order dependence suggested by earlier workers) indicates that additional data points are needed to clarify the situation. This can be accomplished by evaluating the changes in reaction rate with four and/or eight times as much hydrogen present as have been used so far.

It is also possible that the data points in Fig. 14 can be explained from pore volume and surface area measurements. Further refinement of our model is expected as more data are obtained regarding the char's structural changes upon reaction.

C. Relation of Surface Area and Porosity of Hanna Char to the Extent of Gasification

Investigations of the reaction of steam with chars prepared from Hanna subbituminous coal (reported in earlier reports of this series) indicated a strong dependence of the reaction rate on the amount of carbon that had been gasified from the sample. Generally, the maximum rate of reaction was not attained until at least 50% of the carbon had been gasified. A typical plot of the observed reaction rate *vs.* percent carbon gasified is shown in Fig. 16. Under these conditions (750°C, 2.7-atm steam partial pressure), the maximum reaction rate was observed after approximately 70% of the carbon had been removed, and the initial reaction rate was less than one-third the maximum rate. This phenomenon led us to postulate that the pore structure of this char is very poorly developed in the fresh char, and that before the maximum reaction rate could be attained, pores of sufficient size to permit diffusion of steam and product gases through the char had to be formed.

The purpose of this study was to determine the relationship of pore structure and surface area to the extent of carbon gasification for chars, using gasification conditions typical of those encountered in underground gasification.

Char samples were prepared from Hanna No. 1 coal, using our standard pyrolysis conditions (*i.e.*, a heating rate of 3°C/min to the desired gasification temperature, in a flowing atmosphere of 20% hydrogen in nitrogen at an overall pressure of approximately eight atmospheres). Fresh char (no gasification) was studied, as well as chars from which various fractions of carbon had been removed by steam gasification (at a partial pressure of steam of approximately 2.5 atm). For chars pyrolyzed at 750°C, five samples were obtained: fresh char and chars from which 4.5, 14.7, 37.9, and 65.1% of the carbon had been gasified. A series of chars was also pyrolyzed at 600°C, but their gasification rates were so low that the maximum amount of

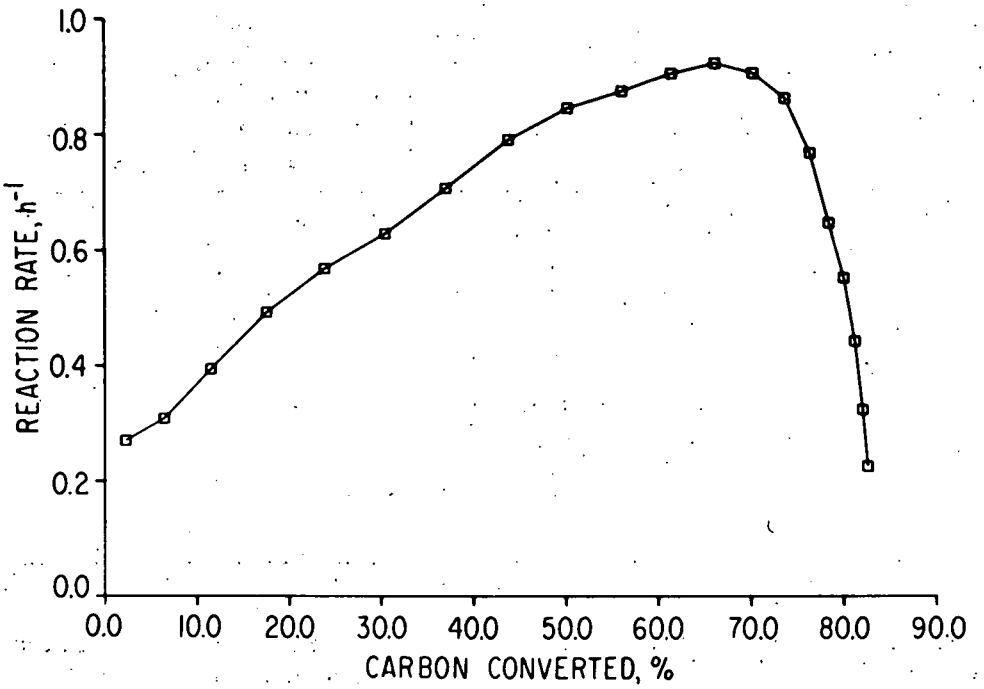

Fig. 16. Reaction Rate *vs.* Percent Carbon Conversion for Hanna No. 1 Char, 750°C, 275 kPa (2.75 atm) Steam. ANL Neg. No. 308-78-466

carbon removed from the char samples was only 31.4%. The samples of 600°C char studied were: fresh char and chars from which 3.1, 9.3, 22.3, 25.3, and 31.4% of the carbon had been removed.

These char samples were submitted for surface area measurements by nitrogen (BET) adsorption and for pore structure determination.

The pore structure determinations were carried out using an Aminco mercury porosimeter. This instrument measures the distribution of pore sizes for pores with diameters larger than 60 Å. The total volume of pores with diameters smaller than 60 Å could be determined by comparing the apparent density of the char samples measured in the porosimeter at 30,000 psig with the true density of the char measured in a helium pycnometer. A helium pycnometer was obtained during the month of September, but was not available for use during this study.

The results of surface area measurements are summarized in Table 3. The reason for the decrease in surface area for the 600°C sample with 3.1% of the carbon removed is not known, but it is obvious that in general, surface area increases rapidly as carbon is removed. It is interesting that at 600°C, the surface area begins to decrease when more than 25% of the carbon is gasified, but at 750°C, surface area does not begin to decrease until approximately 60% of the carbon has been removed.

Table 3. Surface Areas of Hanna Chars

Pyrolysis and Gasification Temperature, °C	Carbon Removed, %	Surface Area, m^2/g	Pyrolysis and Gasification Temperature, °C	Carbon Removed, %	Surface Area, m^2/g
600	0	25.1	750	0	45.8
	3.1	10.5		4.5	109
	9.5	273		14.7	169
	22.3	324		37.9	286
	25.3	314		65.1	203
	31.4	141			

Figure 17 shows a comparison of the pore structures determined for the 750°C char as the carbon is gasified. The fresh char has essentially no pores with volumes larger than 300 Å. However, as carbon is removed from the char, the pore volume increases quickly and is still increasing with 65% of the carbon removed. In Fig. 18, the dependence of pore volume on percent carbon gasified is shown for ranges of pore sizes. At the gasification conditions used, the total volume of pores with diameters larger than 10,000 Å does not

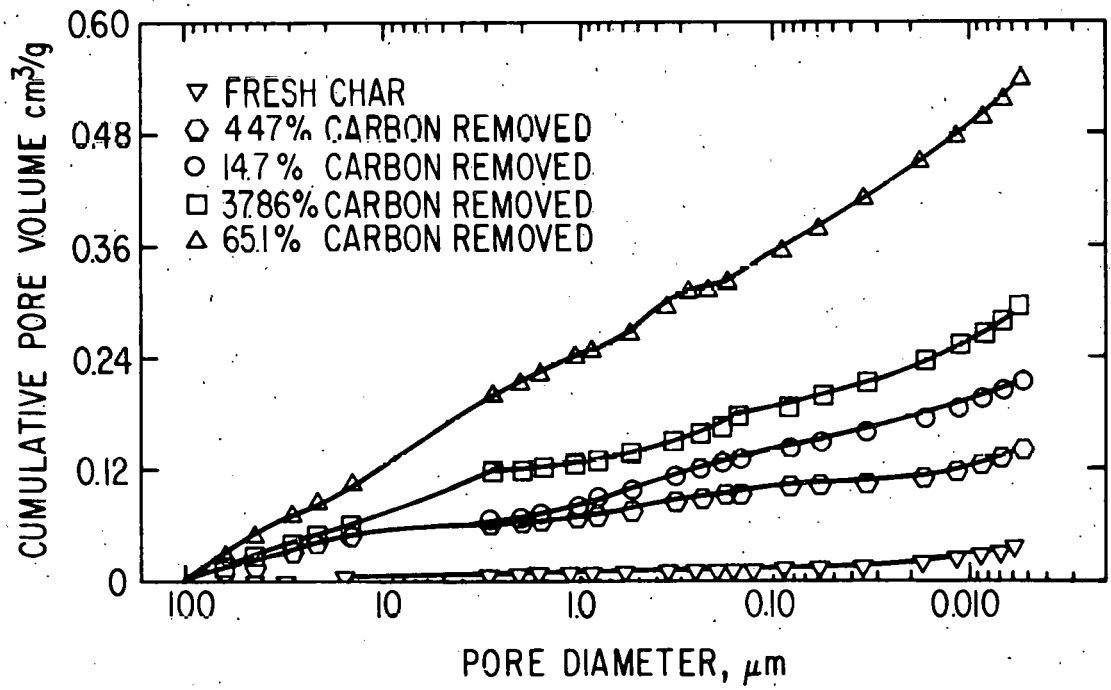

Fig. 17. Pore Volume Distribution in Hanna Char Prepared and Gasified at 750°C

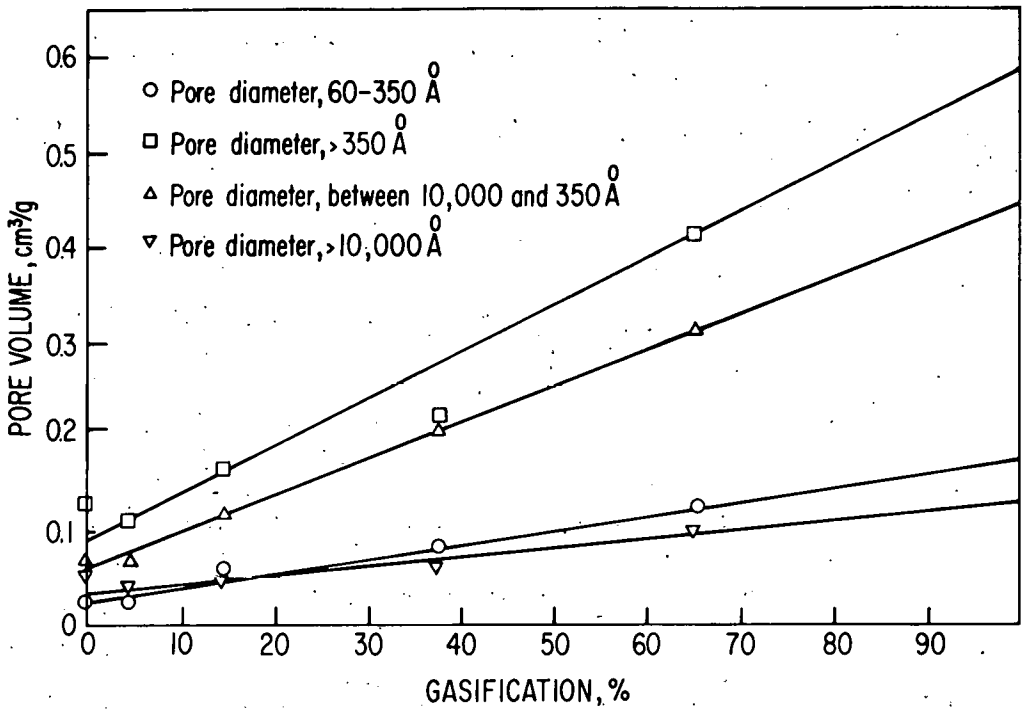

Fig. 18. Pore Volume *vs.* Percent Carbon Gasified. Hanna Char, 750°C.

increase significantly as carbon is removed. This is also true for pores having diameters between 60 and 350 Å. The greatest increase in pore volume is obtained in the intermediate sized pores having diameters between 350 and 10,000 Å.

In Fig. 19, we see a completely different pattern for chars prepared and gasified at 600°C. Figure 19 shows the relationship between total pore volume (*i.e.*, pores with diameters >60 Å) and the percent carbon removed. For these chars, the pore volume remains relatively constant until approximately 25% of the carbon has been removed, after which the pore volume increases quite rapidly. Figure 20 shows a similar relationship for pores with diameters larger than 350 Å although the increase in pore volume appears to begin at approximately 20% carbon removal. However, as shown in Fig. 21, pores with diameters between 60 and 350 Å begin developing immediately upon onset of gasification. This would be expected for a char which initially contains only pores having very small diameters. The helium density measurements still to be carried out are expected to confirm this.

Since the reaction rate for steam and char at 600°C increases approximately linearly as a function of carbon removal until approximately 50% of the carbon is removed (Fig. 22), it appears that attainment of a maximum reaction rate at this low temperature depends on the development of pores in the 60 to 350 Å diameter range, rather than the development of pores with diameters larger than 350 Å. However, at higher temperatures with correspondingly higher reaction rates, maximum reaction rates will be attained only if larger pores are developed to accommodate the greater flows of steam and reaction products.

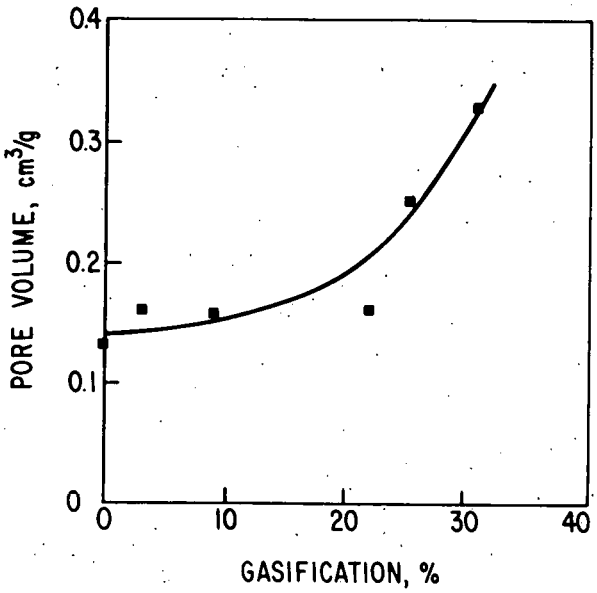

Fig. 19. Volume of Pores with Diameter Larger than 60 Å *vs.* Percent Gasification. Hanna Char, 600°C

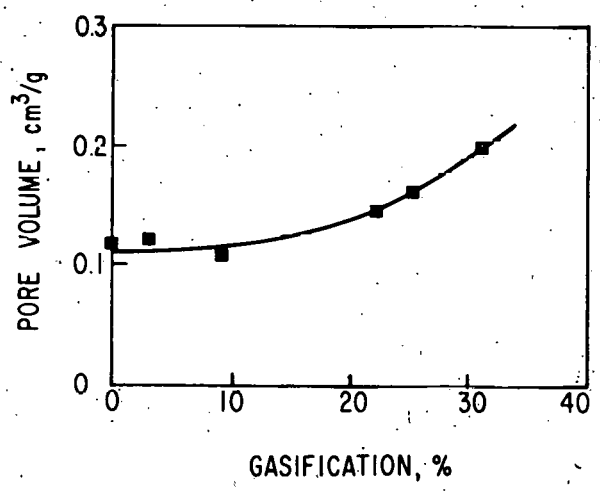

Fig. 20. Volume of Pores with Diameters >350 Å *vs.* Percent Gasification. Hanna Char, 600°C.

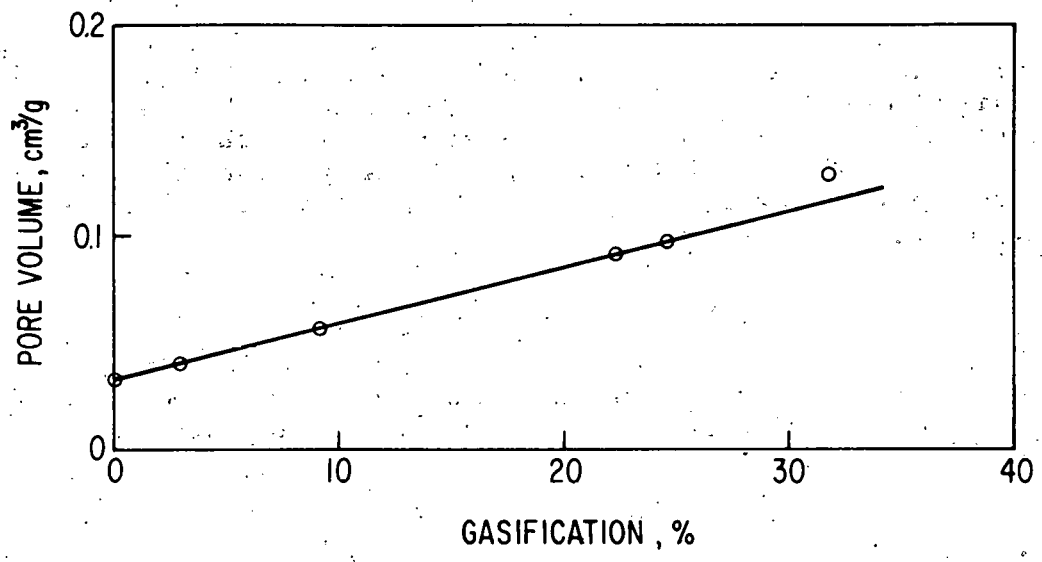

Fig. 21. Volume of Pores with Diameters of 60-350 Å *vs.* Percent Gasification. Hanna Char. 600°C

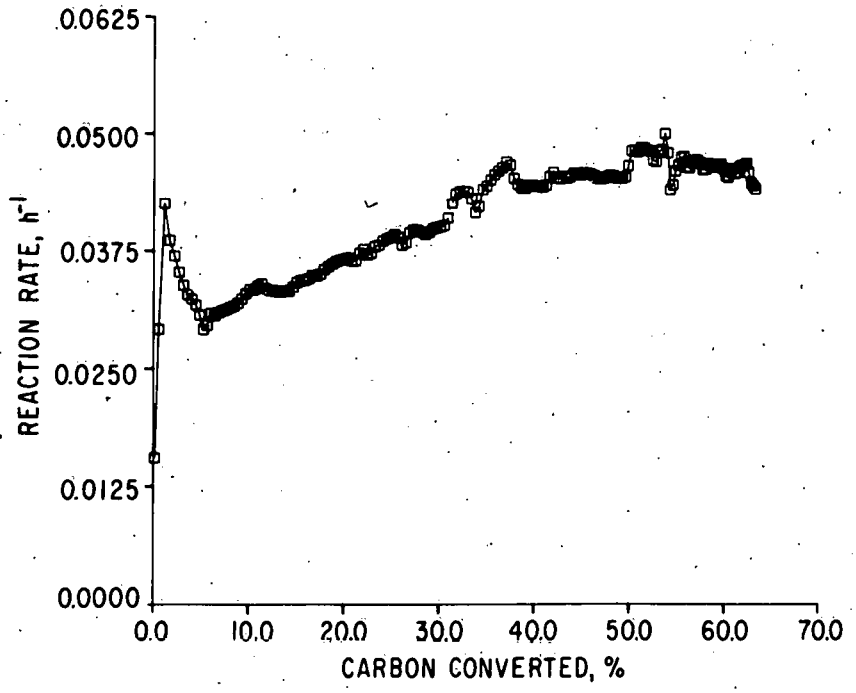

Fig. 22. Instantaneous Carbon Conversion Rate for Hanna No. 1 Char, 600°C, 268 kPa (2.68 atm) Steam, Run 86

Since a decrease in surface area as a function of X_c is not accompanied by a similar drop in reaction rate, structural variation of char pores may have an additional influence. Furthermore, it appears that neither the measured pore volumes nor the surface areas alone exhibit the dependence on X_c found to best fit the reaction rate (Eq. 16). At present, the relationship between the physical changes occuring during gasification and their influence on reaction rate is expressed as:

$$f(X_c,T,P_i,....) = X_c^{0.59} \qquad (16)$$

Until more information is obtained on the surface area and pore structure variation, the above expression will be used as part of our rate model for Hanna subbituminous coal.

REFERENCES

1. J. Fischer, J. E. Young, R. N. Lo, D. C. Bowyer, J. E. Johnson, and A. A. Jonke, *Gasification of Chars Produced Under Simulated In Situ Processing Conditions, Annual Report, October 1975—September 1976,* Argonne National Laboratory Report ANL-76-131 (December 1976).

2. J. Fischer, J. E. Young, J. E. Johnson, and A. A. Jonke, *Laboratory Support for In Situ Gasification--Reaction Kinetics, Annual Report, October 1976—September 1977,* Argonne National Laboratory Report ANL/CEN/FE-79-1.

3. H. F. Johnstone, C. Y. Chen, and D. S. Scott, *Kinetics of the Steam-Carbon Reaction in Porous Graphite Tubes,* Ind. Eng. Chem. *44*(7), 1564 (1952).

4. J. D. Blackwood, *The Kinetics of Carbon Gasification,* Coke Gas *22,* 250 (1960).

5. J. Gadsy, C. H. Hinshelwood, F. R. S., and K. W. Sykes, *The Kinetics of the Reactions of the Steam-Carbon System,* Proc. R. Soc. London *A187,* 129 (1946).

6. J. L. Johnson, *Kinetics of Bituminous Coal Char Gasification with Gases Containing Steam and Hydrogen,* Adv. Chem. Ser. *131,* 145 (1954).

7. J. M. Pilcher, P. L. Walker, Jr., and C. C. Wright, *Kinetic Study of the Steam-Carbon Reaction,* Ind. Eng. Chem. *47*(9), 1742 (1955).

8. J. Fischer, J. E. Young, J. E. Johnson, D. C. Bowyer, and A. A. Jonke, *Laboratory Support for In Situ Gasification Reaction Kinetics, January—March 1977,* Argonne National Laboratory Report ANL/CEN/FE-77-2.

Distribution for ANL/CEN/FE-79-4

Internal:

W. E. Massey
J. Fischer
W. Podolski
A. A. Jonke
D. S. Webster
L. Burris
A. Tevebaugh
S. Wong
G. M. Kesser
P. R. Fields
J. Royal
J. E. Young (20)
J. E. Johnson
L. Cuba
J. W. Simmons
H. Huang
S. Lee
A. B. Krisciunas
ANL Contract File
ANL Libraries (5)
TIS Files (6)

External:

DOE-TIC, for distribution per UC-90c (278)
Manager, Chicago Operations and Regional Office, DOE
Chief, Office of Patent Counsel, DOE-CORO
President, Argonne Universities Association
Chemical Engineering Division Review Committee:
- C. B. Alcock, U. Toronto
- R. C. Axtmann, Princeton U.
- J. T. Banchero, U. Notre Dame
- T. Cole, Ford Motor Co.
- P. W. Gilles, U. Kansas
- R. I. Newman, Warren, N. J.
- H. Perry, Resources for the Future, Washington
- G. M. Rosenblatt, Pennsylvania State U.
- W. L. Worrell, U. Pennsylvania

S. Akhtar, Pittsburgh Energy Technology Center (6)
S. Alpert, Electric Power Research Inst.
C. Bagge, National Coal Association, Washington
J. S. Ball, Bartlesville Energy Technology Center
R. M. Boyd, Laramie Energy Technology Center
C. F. Brandenburg, Laramie Energy Technology Center
J. A. Brooks, Amoco Oil Co., Naperville, Ill.
E. L. Burwell, Div. of Fossil Fuel Extraction, USDOE
J. Butt, Northwestern U.
G. W. Douglas, U. Alabama
V. Dranoff, Northwestern U.
T. F. Edgar, U. Texas at Austin
D. Fischer, World Energy, Inc., Laramie
J. F. Flagg, Universal Oil Products Co.
P. Fulton, U. Pittsburgh
R. Giberti, Kennecott Copper Corp., Lexington, Mass.
R. Gunn, Laramie Energy Technology Center
O. J. Hahn, U. Kentucky
R. G. Hickman, Lawrence Livermore Lab.
G. Hill, Electric Power Research Inst.
J. Jennings, Texas A&M U.
W. S. Jones, Div. of Fossil Fuel Processing, USDOE (3)
G. Long, Northern Illinois Gas Co., Aurora, Ill.
R. M. Lundberg, Commonwealth Edison Co., Chicago
P. S. Lykoudis, Purdue U.
J. W. Martin, Morgantown Energy Technology Center

M. D. McKinley, U. Alabama
G. A. Mills, Div. of Planning and Systems Engineering, USDOE
J. Nichols, Oak Ridge National Lab.
J. Pasini III, Morgantown Energy Technology Center
W. H. Peters, Massachusetts Inst. of Technology
A. A. Pitrolo, Morgantown Energy Technology Center
J. W. Ramsey, Div. of Fossil Fuel Extraction, USDOE
B. Rubin, Lawrence Livermore Lab.
P. Russell, Denver Mining Research Center
A. F. Sarofim, Massachusetts Inst. Technology
J. G. Savins, Mobil R&D Corp., Dallas
F. Schora, Inst. of Gas Technology, Chicago
L. A. Schrider, Morgantown Energy Technology Center
A. P. Sikri, Div. of Fossil Fuel Extraction, USDOE (2)
S. J. Spataro, Lawrence Livermore Lab.
M. Steinberg, Brookhaven National Lab.
D. R. Stephens, Lawrence Livermore Lab.
K. Street, Lawrence Livermore Lab.
L. D. Strickland, Morgantown Energy Technology Center
Tetra Tech, Inc., Arlington, Va.
U. S. Bu. Mines, Director, Pittsburgh
N. Vanderborg, Los Alamos Scientific Lab.
C. W. Whitten, Peabody Coal Co., Columbia, Tenn.
W. Wiser; U. Utah
D. Zallen, Energy and Environmental Research Corp., Santa Ana
S. H. Zukor II, Div. of Fossil Fuel Extraction, USDOE